Selection of suitable surfactants for the incorporation of organic liquids into fresh geopolymer pastes

Christel Pierlot, Hanyu Hu, Charles Reeb, Jordan Bassetti, Matthieu Bertin, David Lambertin, Catherine Davy, Véronique Rataj

Selection of suitable surfactants for the incorporation of organic liquids into fresh geopolymer pastes

Christel Pierlot[a,*], Hanyu Hu[a], Charles Reeb[a,b], Jordan Bassetti[a], Matthieu Bertin[b], David Lambertin[b], Catherine Davy[a], and Véronique Nardello-Rataj[a]

[a] Centrale Lille, Université de Lille, CNRS, Université Artois, UMR 8181-UCCS-Unité de Catalyse et Chimie du Solide, Lille, France.

[b] CEA, DES, ISEC, DE2D, SEAD, LCBC, Univ Montpellier, Marcoule, France.

Abstract

Geopolymers (GP) have recently emerged as suitable binders for the conditioning of radioactive organic liquids (OL). The condition for suitably incorporating high amounts of OL into GP is assessed in this research. A series of OL has been selected, comprising alkanes (dodecane and 2 paraffinic mineral oils), an industrial gear oil and tributylphosphate (TBP), in order to cover a wide range of viscosities (0.0018 to 2.33 Pa.s). The incorporation of viscous OL (> 0.2 Pa.s) into fresh GP results in a regular torque increase, indicating a suitable process with the dispersion of the OL in the form of fine micrometric droplets. When the torque remains stable, for OL of low viscosity (< 0.2 Pa.s) like TBP/Dodecane mixtures, the incorporation is not possible, or only partial in the form of large droplets quickly coalescing and leading to an organic supernatant above the hardened GP.

For low viscosity OL, surfactants are required. The use of quaternary ammoniums (QAs) like cetyltrimethylammonium bromide (CTAB) has been studied. Torque monitoring shows that the OL is incorporated similarly in the GP slurry, whether the surfactant is introduced at the beginning, through the course or at the end of the mixing process. The torque evolution also provides the optimum surfactant concentration, by evidencing that beyond a certain concentration, the medium hardens too quickly, preventing the incorporation of OL. Finally, torque monitoring highlights that QAs with shorter alkyl chains, such as hexamethyltrimethylammonium, are able to replace CTAB with the same efficiency. Therefore, the powerful action of CTAB on the incorporation of alkanes into GP is attributed to its positive charge rather than to its surfactant effect.

1. Introduction

Oil incorporation into geopolymer suspensions

Geopolymers (GP) are inorganic aluminosilicate materials synthesized at room temperature by the activation of a solid aluminosilicate precursor (e.g. metakaolin, fly ash F) in alkaline conditions (fresh GP) ((((Davidovits, 1991; Provis et al., 2009)))) .The resulting mixture hardens to form a solid material (hardened GP). Mixing organic liquids (OL) with such aqueous suspensions (Bai and Colombo, 2018; Davidovits, 1991; Duxson et al., 2007; Provis et al., 2009) has been recently described for the synthesis of porosity-controlled media, thermal insulating foams or filtration supports (Bai et al., 2016; Barbosa et al., 2018; Cilla et al., 2017; Glad and Kriven, 2015; Medpelli et al., 2014)⁻ and for the treatment of radioactive wastes (Cantarel et al., 2018, 2015). Vegetable oils (Bai et al., 2016; Cilla et al., 2017) were also used as the organic phase. Because of the strong alkaline medium, the triglycerides contained in the vegetable oils are converted into glycerol and sodium salt of carboxylic acids, which act as surfactants during GP stirring. Therefore, unlike OL containing alkanes, incorporation of vegetable oils into aqueous geopolymer suspensions does not cause any process issue.

Two-steps oil incorporation process

With the aim of immobilizing radioactive organic wastes, alkanes (Cantarel et al., 2018; Lambertin et al., 2018) and paraffin oil (Liu et al., 2018) have been used as model oils. In (Cantarel et al., 2018; Lambertin et al., 2018), the two-steps incorporation process first requires the formulation of an oil in alkaline water emulsion at high shear rate in a first reactor, followed by its incorporation into an aqueous and viscous metakaolin suspension in a second reactor. Even if this process allows an efficient incorporation up to 20%v of OL in GP, by providing oil droplets of about 10 to 100 μm, this two-steps protocol is hardly applicable at the industrial scale.

Moreover, the surfactant choice to form the initial emulsion is critical, since this conditions not only the stability of the emulsion, but also the easiness of incorporating the emulsion in the GP suspension. Among the different surfactants that have been tested, alkyl quaternary ammoniums, and in particular cetyl trimethyl ammonium bromide (CTAB), appears as a promising emulsifier. When using CTAB, the viscosity of the fresh hexadecane/geopolymer composite pastes at 20% by volume of hexadecane is between 100 and 1000 times greater than the viscosity of the fresh geopolymer free from alkane (Cantarel, 2016).

One-step oil incorporation process

Former studies highlight that when paraffin oil is dispersed into a GP slurry, the suspension is not stable with time (Thakur et al., 2019). However, it is worth noting that it is possible to incorporate motor oils (Cantarel et al., 2015; Davy et al., 2019) in a GP cement directly, in a one step process, without using any surfactant. Even if no details are given concerning the composition of these industrial oils, which probably contain additives like surfactants with some emulsifying and/or stabilizing properties, it was the first time that a one-step process had been successfully used. Cantarel et al. (Cantarel et al., 2015) noted an increase in viscosity during the incorporation of the oil.

Offline rheological measurements

Most of the time, rheological measurements are performed offline, which requires to transfer the fresh GP from the reactor to the measurement cell of the rheometer. The rheological properties of these fresh pastes are generally determined using rotational rheometers with a parallel plate (Sun et al., 2020), a cone plate (Dusserre et al., 2020) or a bowl with an helical steel ribbon impeller (Steins et al., 2012) type geometry. Offline rheological measurements can be carried out using several sample solicitations. As an example, by simply measuring the evolution of viscosity versus time on a scale of several hours, the setting time of geopolymers can be estimated (Autef et al., 2013).

Moreover, typical rheological shear stress/shear rate curves also provide apparent viscosity, yield stress and plastic viscosity. In Sun et al. (Sun et al., 2020), these last two basic parameters have been characterized to determine to what extent geopolymers meet the requirements for extruding and molding processes.

In Dusserre et al. (Dusserre et al., 2020), thixotropic curves of fresh geopolymers have been studied using a cone plate geometry. From the interpretations of the rheological changes with time, a model for the dissolution mechanism of metakaolin followed by polycondensation is proposed.

Oscillatory rheological experiments allow the determination of viscoelastic parameters (G', G'', and tan δ). With these information, Steins et al. (Steins et al., 2012) have shown that a rigid percolating network in fresh GP occurs more quickly with alkali activator. Hussain et al.

(Hussain et al., 2005, 2004) have shown that the relaxation strength (tan δ) is correlated to the glass transition temperature (Tg) of geopolymer-modified composites. In Rouyer et al. (Rouyer and Poulesquen, 2015), the elastic and viscous moduli are also measured to investigate the percolation and aggregation mechanisms during geopolymer paste hardening.

Online rheological measurement

To our knowledge, there are not many articles dealing with on line rheological measurement, and even less when it is related to oil incorporation in fresh geopolymer.

In some cases (Autef et al., 2013), rheological measurements are performed using an unconventional geometry to facilitate mixing, using a bowl and a helical steel ribbon impeller. In that case, the torque measured during stirring can be converted to a viscosity thanks to a preliminary calibration, performed with standard oils (Autef et al., 2013). However, geopolymer pastes may exhibit high stiffness and cohesion, which makes common shear-driven rheometers inappropriate. In that case, a homemade small-scale ramp-type rheometer has been used to simulate an extrusion process and to convert the applied pressure (i.e. the resulting torque) to the rheological behavior of the pastes (Yunsheng et al., 2008).

Online torque measurements have already been used to follow emulsification processes of viscous organic polymers such as epoxy resin (Akay, 1997), polyethylene (Akay and Tong, 2001), polyester (Catte et al., 2018; Pierlot et al., 2018), polyurethane (Saw et al., 2004), rosin resins (Song et al., 2011), silicon resin (Galindo-Alvarez et al., 2011), bisphenol A-polyester (Goger et al., 2015) or bitumen (Edward et al., 2014). The torque may be converted to viscosity by calibration curves or by mathematical models (Allouche et al., 2004; Edward et al., 2014; Song et al., 2011).

In this article, the aim is to take advantage of the high viscosity of fresh geopolymers to perform online torque tracking into the reactor before and during organic liquid incorporation. The objective is to determine to what extent torque tracking provides relevant information on both the process of oil incorporation and its repartition into the GP. A series of organic liquids (OL) have been selected for this study, comprising alkanes (dodecane, 2 paraffinic mineral oils (Finavestan and Nevastane)) as well as an industrial motor oil (Shellspirax) and tributylphosphate (TBP), in a view of covering a wide range of viscosity (0.0018 to 2.33 Pa.s).

The effects of different quaternary ammoniums on the oil incorporation have been studied, including the well-known cetyltrimethylammonium bromide (CTAB), with the aim of confirming the positive effect of CTAB on the organic liquid incorporation.

2. Materials and methods

2.1. Chemicals

Geopolymers with the following molar composition 3.8 SiO_2 : 1 Al_2O_2 : 1 Na_2O : 13 H_2O were synthesized using a sodium silicate solution (Woellner, Betol® 39 T: 27.8 wt% SiO_2, 8.3 wt% Na_2O and 63.9 wt% H_2O), sodium hydroxide (Sigma Aldrich, 99%) and an aluminosilicate source (metakaolin, ARGICAL-M 1000, Imerys). Metakaolin was chosen in this study for its stable chemical composition and easy supply, which is not the case of other raw materials used for geopolymer formulation (e.g. fly ash F, red mud).

Hexa, tetra, dode, de, octa, hexa-decylltrimethylammonium bromide and Sudan IV were purchased from Sigma-Aldrich. Mineral oils Nevastane EP100 and Finavestan A360B were obtained from Total, Shellspirax S2 A 80W-90 is a commercially available oil, Dodecane, and Tributyl phosphate were purchased from VWR with an announced purity of 99%. Chemicals were used as received without any further purification. Water was deionized using a Milli-QR©Water Purification System and was collected with a resistivity $\geq$ 18.2 MΩ·cm.

2.2. Propeller and reactor

The stirring system is a propeller (Table 1) with three contiguous blades (6.0 cm diameter) fixed on a stainless steel rod (0.6 cm diameter). The reactor is a cm beaker with an internal diameter of 8.0 cm. During the mixing step, the propeller is placed at 1 cm from the bottom of the beaker.

2.3. Geopolymer/oil preparation

First, 12.92 g of sodium hydroxide, 82.16 g of Betol® 39 T silicate solution and 11.04 g of deionized water are introduced into a 500 mL reactor to form the activating solution: The mixture was first stirred at 400 rpm with the Heidolph RZR 2051 control to ensure the complete dissolution of sodium hydroxide, and then allowed to cool down to room temperature during 1 hour. Afterwards, 72.12 g of ARGICAL-M 1000 are added during 2 min and the mixture is stirred at 800 rpm during 15 min until both visual homogeneity of the dispersion and torque stability. At this stage, the fresh geopolymer paste is obtained. The last step consists of introducing the organic liquid colored with Sudan IV into the reactor at a flow rate of 4.0 ml.min^{-1} with a Syringe pump Legato (kdScientific). The organic liquid is introduced into the geopolymer paste so that the point of impact is located at equal distance from the center and the periphery of the beaker. The fresh mixture (called fresh "geoil") is poured into graduated test tubes for liquid state characterization (discussed below) or directly transferred into open

cylindrical polystyrene containers and aged at room temperature for 2 days before solid-state characterization.

2.4. Rheological experiments

3 mL of the liquid geopolymer suspension is placed in the gap of a cone-plate (6 cm, 4°) Kinexus rheometer (Malvern). A shear stress gradient from zero to the maximum value (Pa), chosen in accordance to the consistency of the sample, is applied in 1 min followed by the return in the same conditions, in order to reach at least a shear rate of 100 s^{-1}. Experiments were carried out at a constant temperature of 25.0 °C. The linear profiles obtained allow the determination of the viscosity (shear stress divided by shear rate) in the studied scale.

2.5. Torque measurements

The torque is measured in function of time using a Heidolph RZR 2051 control at a selected stirring rate (100 to 800 rpm) and recorded via a specific software (Watch/Control 200) provided by Heidolph.

2.6. Optical microscopic analysis

Optical microscopic observations are carried out using an Axiostar microscope Zeiss in transmission-mode for fresh geopolymers. Due to their important opacity, geopolymer suspensions are directly diluted with water (1/10) on the small glass plate before observation. A Keyence VHX-5000 microscope is also used in reflection-mode for hardened geopolymer observations..

2.6. Zeta potential

10 mg of metakaolin and an appropriate amount of alkyl trimethyl ammonium bromide are dispersed in 10 mL of aqueous solutions for 5 min using ultrasonic waves and left for 12 hours at rest. The pH of the aqueous solutions is adjusted by the addition of sodium hydroxide or hydrochloric acid and controlled before the Zeta Potentiel analysis, which is performed using a Nanosizer Malvern instrument.

2.7. Washburn tests

Washburn tests are carried out using a Krüss Force Tensiometer - K100 in combination with Krüss Windows based Laboratory Desktop software in the sorption mode. 1.0 g of (natural or hydrophobically modified) metakaolin is placed in an appropriate sample holder, packed for 30

seconds using 2 kg weight and finally suspended from the balance in the tensiometer. The liquid is raised until it just touches the bottom of the porous sample and mass^2 (w^2) versus time (t) data are then collected as liquid penetrates into the solid.

Hydrophobically metakaolin powders were obtained as follow: 5.0 g of natural metakaolin were introduced in 50 mL of 10^{-2} M CTAB aqueous solution of and let for stirring during 2 hours. The powders were then filtered on paper and dried in an oven at 60 °C overnight.

3. Results and discussion

## 3.1. Torque/Viscosity correspondence

The selected organic liquids (OL) of interest comprising alkanes (dodecane, 2 paraffinic mineral oils (Finavestan and Nevastane) as well as an industrial motor oil (Shellspirax) and tributylphosphate (TBP) have been first analyzed by shear stress/shear rate rheological curves. Viscosity profiles are presented in Fig. 1. A. The maximum shear stress applied is selected in order to reach 100 s^{-1} that could be representative of a mean shear rate generated in the reactor during fresh geopolymer mixing.

The tested OLs are almost Newtonian since their viscosity is relatively constant with the shear rate. The small variations in viscosity for extremely flowing OLs (water, dodecane, TBP) at low speed gradients (< 10 s^{-1}) are due to experimental conditions. The viscosity at 100 s^{-1} (Table 1) versus the torque obtained in the reactor at different speed rates have been plotted (Fig. 1. B).

Table 1. Viscosity at 25 °C measured at 100 s^{-1} for different organic liquids, fresh geopolymer pastes with and without incorporated Shellspirax oil (20%v) and p ratio (viscosity of OL/ viscosity of fresh GP).

Organic liquids	Viscosity at 100 s^{-1} at 25 °C (Pa.s)	p ratio (viscosity of OL/ viscosity of GP)
Suspension of fresh geopolymer		
with 20%v Shellspirax	5.59	
alone	1.92	
Organic liquid		
Nevastane oil	2.33	1.214
Shellspirax oil	0.32	0.167
Finavestan	0.13	0.068
Tributyl phosphate (TBP)	0.0036	0.002
Dodecane	0.0018	0.001

In order to extend the viscosity/torque correlation curve with more consistent fluids, data obtained with fresh geopolymers (1.92 Pa.s) and with 20%v of Shellspirax oil incorporated (5.59 Pa.s) have been added in Fig. 1. B. For very fluid media (< 0.2 Pa.s), the torque only slightly varies whatever the stirring speed (from 100 to 800 rpm). Thus, the correlation between viscosity and torque is not relevant for OL of viscosity lower than 0.2 Pa.s. For low speeds of rotation (100 or 200 rpm), the torque only increases by 10 N.mm when the viscosity rises from 0.1 to 5.0 Pa.s. On the other hand, at 800 rpm, a large torque amplitude of more than 50 N.mm is observed. Fig. 1. B. shows that a mixing speed of 800 rpm is well adapted to both ensure a good mixing of the geopolymer and to follow the torque evolution during OL incorporation.
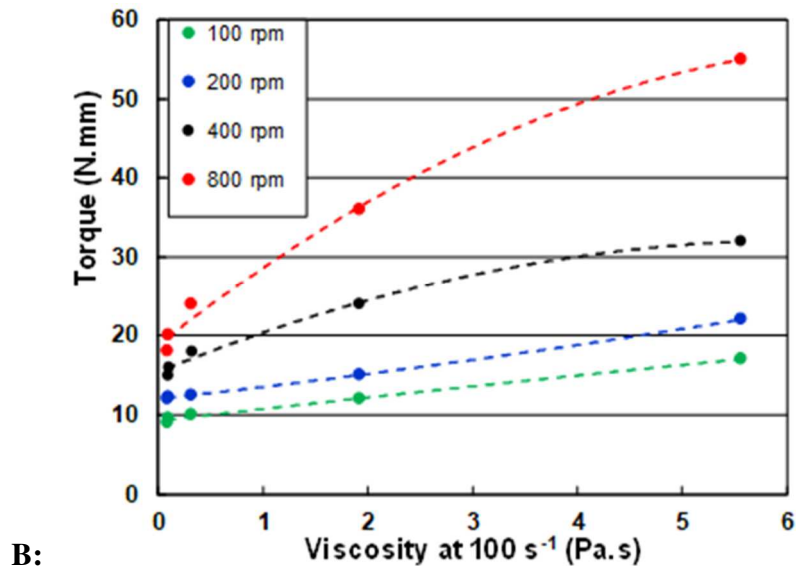

A:

B:
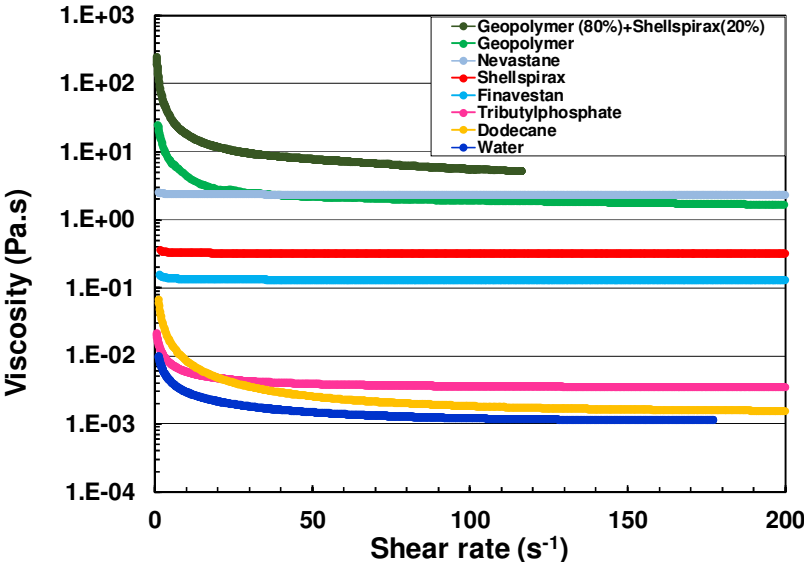
Fig. 1. A: Viscosity (Pa.s) versus shear rate (s^{-1}) measured at 25.0 °C for water, different organic liquids, fresh geopolymers (with 0%v and 20%v of incorporated Shellspirax oil). Viscosity curve have been obtained during increase in shear stress from 0 to σ$_{max}$ during 1 min. σ$_{max}$ is fixed in order to obtain a maximum shear rate around 100 s^{-1}. **B**: Correspondence between viscosity at 100 s^{-1} and torque (N.mm) at different stirring speeds (100, 200, 400 and 800 rpm).

3.2 Choice of geometry / transferability to other mixing geometries

Different stirring propeller (vortex, anchor, dispersing homogonising blades) have been tested without success. Only the propeller with three contiguous blades made it possible to incorporate organic liquids with a minimum speed of 800 rpm. Estimation of Reynold number (Re=23) has been done using Re=N.d^2.ρ/μ with N=13.33 rounds/s (800 rpm), d=6.10^{-2} m, ρ=1672 kg.m^{-3}, m=3.5 Pa.s. Estimation of the maximum shear rate at the extremity of the blade is 151 s^{-1}. Given the high viscosity of the reaction medium, it is important to note that the mixture can be stirred homogeneously as long as the quantity of geopolymer is at a distance from the helix of the order of a few cm. Beyond this distance, the geopolymer at the surface of the reactor is no longer agitated. In the case of an industrial dimensioning, it would probably be necessary to choose more suitable systems with multi-blade systems for example.

3.3. Organic liquids incorporation into fresh geopolymer

The incorporation of OL (Fig. 2) was carried out by always following the same protocol. First, the geopolymer suspension is prepared by adding metakaolin to the activating solution. Once the torque value is stable, the OL is added at a constant flow rate of 4.0 mL per minute. The

At this stage, the mixture is removed from the reactor and a picture of the fresh GEOIL, fixed on the 6 cm diameter propeller is presented in Table 2.

All the points in Fig. 2 for which there is no OL added (v = 0.0 mL) correspond to the same fresh geopolymer composition, thus the small torque variations (35-40 N.mm) can be attributed to slight position change of the propeller in the reactor. In any case, this difference of 5.0 N.mm is negligible in comparison with the torque variation obtained during OL incorporation.

Three torque evolution profiles can be distinguished in Fig. 2 depending of the type of OL that is incorporated, whose corresponding GEOIL aspect (Type I, II or III) are presented in Table 2 before and after hardening. In the case of dodecane or TBP/dodecane, the torque remains constant. The torque recording was proceeded until introduction of 40 mL of OL, but in fact, the oil incorporation into the GP was not taking place. After stopping the agitation, the organic liquid directly coalesced at the surface of the GP. The small amount of OL that is being incorporated is in the form of big droplets of a few millimeters diameter, as can be seen on the picture of the paste (Table 2, first column). In the end, the paste corresponds practically to the fresh geopolymer in terms of viscosity and is defined as **type I** GEOIL.

In case of TBP and Finavestan, the torque increases regularly up to 54 N.mm and then stabilizes after 22 mL of TBP or 42 mL of Finavestan have been incorporated. This late stabilization results from the limit of incorporation and the appearance of big droplets of oil in the GEOIL that can be seen on the propeller (Table 2, second column). The fresh paste is still a bit too fluid to avoid coalescence of OL droplets on the surface of the geopolymer until the hardening phase. GEOIL **type II** will characterize such systems for which the incorporation of oil is possible in a limited proportion and for which an oil resurgence appears before hardening.

In case of Nevastane and Shellspirax mineral oils, the torque increases constantly even after adding 100 mL of oil (55% oil incorporation) and the dispersion seems macroscopically very homogeneous as shown by the appearance of the GEOIL on the propeller (Table 2, third column). The microscopic state (picture not presented) shows the dispersion of numerous oil droplets ranging from 1.0 to 50 microns. GEOIL **type III** will characterize these fresh geoil with an adapted viscosity after oil incorporation that allows the organic liquid to remain trapped in the solid matrix until the hardening is completed. The green area in Fig. 2 is a schematic

representation of torque variation versus volume of organic liquid that leads to GEOIL **type III**.

Finally, with regards to the OL tested, it seems that if its viscosity is greater than 0.13 Pa.s (at $100 \ s^{-1}$) like Nevastane or Shellspirax oils, the incorporation into geopolymer is properly done. If the viscosity is about 0.13 Pa.s, such as the Finavestan oil, incorporation is possible but only at a limited extent of about 43% and the droplets are relatively big (100 microns). For OL with very low viscosities (lower than 0.004 Pa.) such as TBP, dodecane and their mixtures, incorporation is not possible.
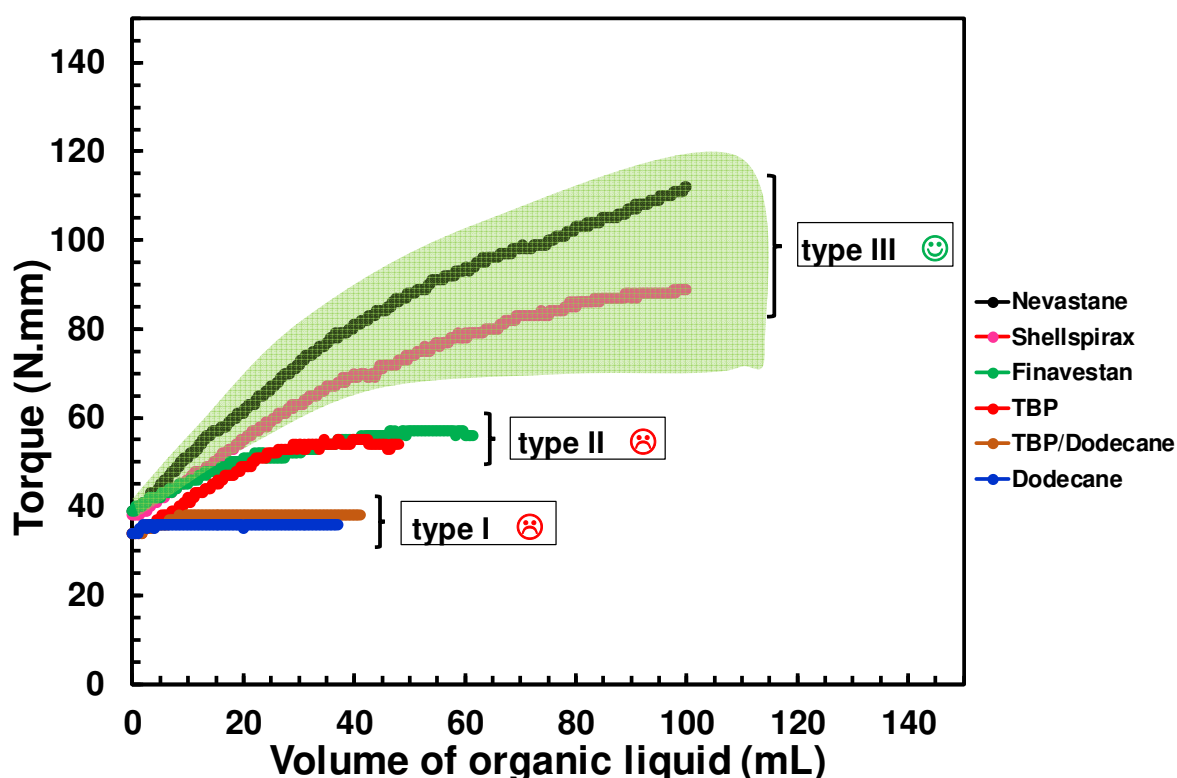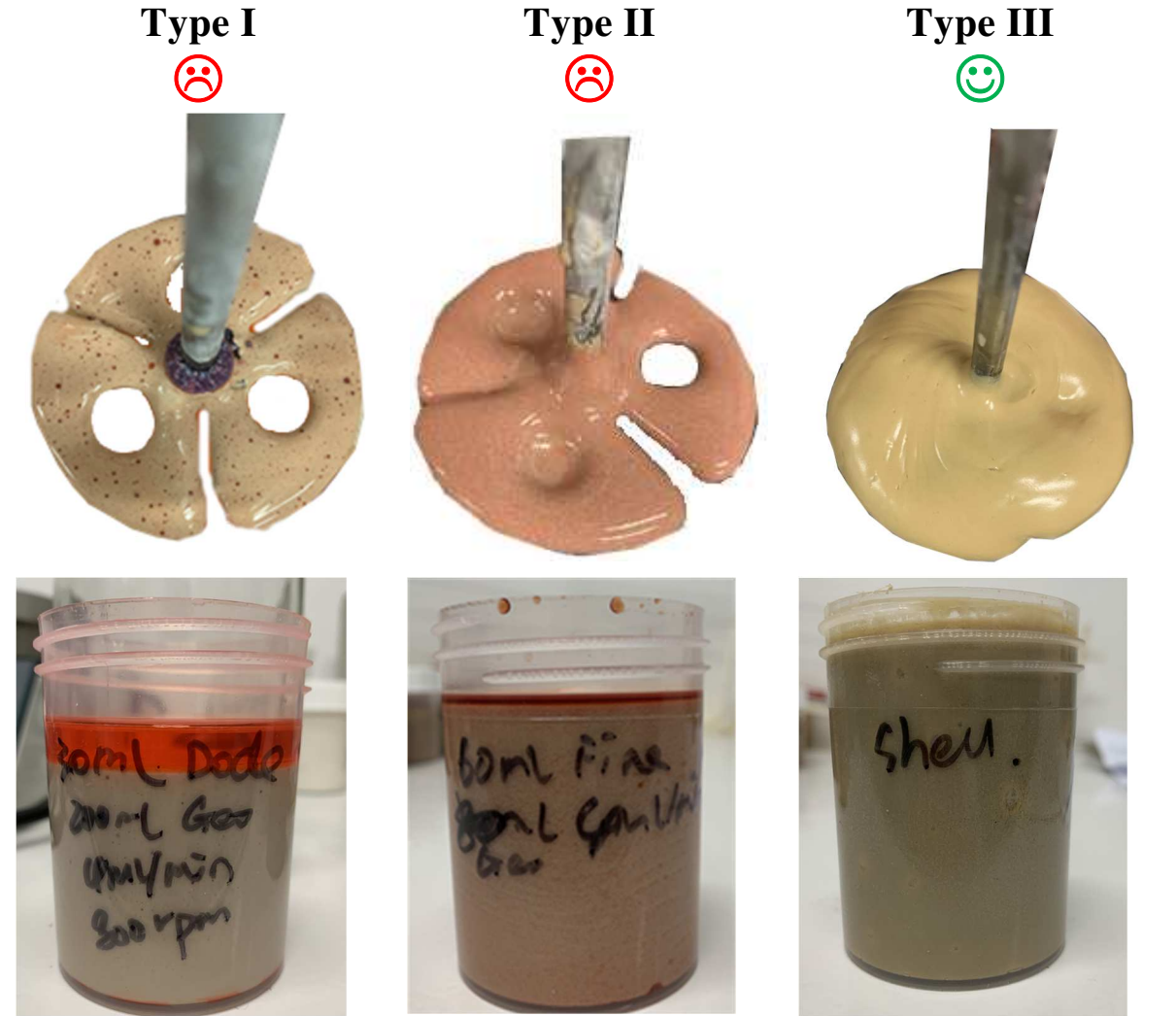

Fig. 2. Torque (N.mm) variation versus volume (mL) of different organic liquids incorporated (flow rate = 4.0 mL.min^{-1} and stirring speed = 800 rpm) into 80.0 mL of fresh geopolymer. Type I, II and III physical aspects of geopolymers are represented in Table 2.

Table 2. Type I, II, III GEOIL before (top) and after (bottom) hardening.

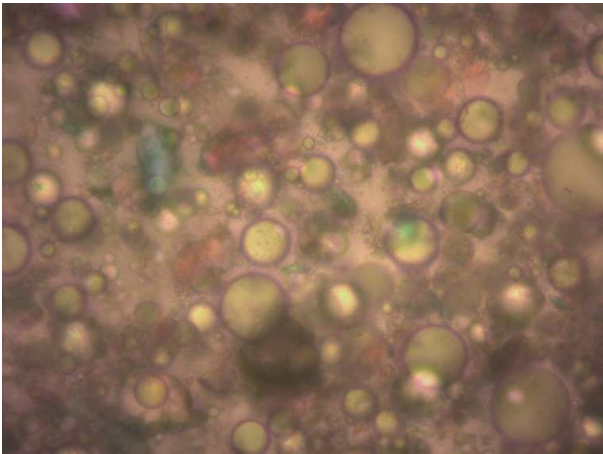| Type I	Type II	Type III
☹	☹	☺

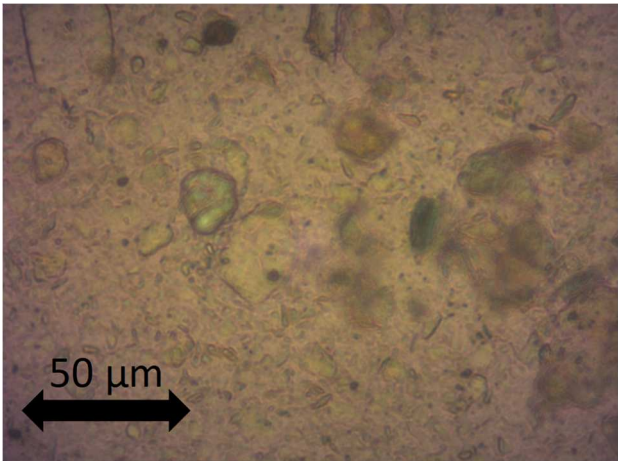**Fig. 3.** Optical microscopy in transmission mode of fresh geopolymer (**A**) and with incorporation of 56% of Shellspirax organic liquid (**B**). Observations have been carried out with preliminary dilution in water (1/10). Small colored (blue, green, red) parts correspond to solid particles that appear under polarized light. Circular oil droplets with sizes ranging from 1.0 to 50 microns are also visible (**B**).

3.3. Effect of the viscosity difference on the incorporation

The effect of the viscosity ratio ($p = \eta_D / \eta_C$) between the dispersed and the continuous phases on the ability of a dispersed liquid to be burst has been studied by Grace (Grace, 1982). This study concluded that there is a range of most favorable ratios ($10^{-2} < p < 3$) to produce a high quality dispersion. It appears that these conclusions are also valid in the present study if the fresh geopolymer is considered as the continuous phase ($\eta_C = 1.92$ Pa.s) and the organic liquid as the dispersed phase. In fact, for Nevastane ($p = 1.2$) and Shellspirax ($p = 0.17$), the oil incorporation is successful (Table 1). For OL with lower p ratio such as Finavestan ($p = 0.13$) and TBP ($p = 0.004$), the incorporation of oil is still possible but at a limited amount, especially in the case of TBP for which the p ratio is outside the good interval conditions ($10^{-2} < p < 3$). As expected, dodecane, which does not incorporate into the geopolymer has indeed the lowest p ratio ($p = 0.002$). Organic liquids with a viscosity high enough to reach a p ratio higher than 3.0 have not been tested in this study. However, Grace's observations might be applicable to geopolymer suspensions with organic liquids having superior viscosities, as observed during the bad dispersion of excessively viscous epoxy liquids into fresh geopolymer resin (Wang et al., 2019).

3.4. Effect of CTAB added at different steps of the process

To see whether the addition of CTAB in geopolymer paste facilitates OL incorporation, Finavestan oil was selected for its moderate incorporation (Type II) without any additives.

In the protocol of the present study, the components are added in the following order: activating solution, metakaolin and oil. The CTAB is introduced at three different steps of the process: directly in the activation solution, just after the addition of metakaolin, or at the end, just after the oil incorporation. The concentration of CTAB (10^{-2} M) was calculated with respect to the volume of the fresh geopolymer. Without CTAB (black and green curves in Fig. 4), the torque typically increases from 35-40 to 55 N.mm during the addition of Finavestan, as already observed in Fig. 2. The optical microscopy visualization of the hardened GEOIL without oil are presented in Fig. 5. A Angular micron particles can be observed that probably corresponds to metakaolin (noted MK in the photo) trapped in the polymerized aluminosilcate matrix. (Fig. 5. B) confirms the presence of large Finavestan oil droplets of more than 50 microns, the reflection of which is materialized by a small white disc in the center of the drop.

The addition of CTAB in the activating solution containing metakaolin already induces an increase in torque (50-55 N.mm) compared to the sample free of CTAB (25-40 N.mm). Oil addition then leads to a strong increase of the torque profile, up to 160 N.mm. After hardening, the microscopic analysis shows a homogeneous size distribution with droplets smaller than 10 microns that can be detected by the numerous small white points (Fig. 5. C). An enlargement of a central portion of the photo in fig. 5. C (see insert) allows the small drops to be seen better.

Even more surprising, when CTAB is added after the incorporation of Finavestan, the torque progressively increases during 10 minutes, leading to a similar torque value (150 N.mm) as when the CTAB is directly introduced in the activating solution. Again, the droplet size is about a few microns (Fig. 5. D).
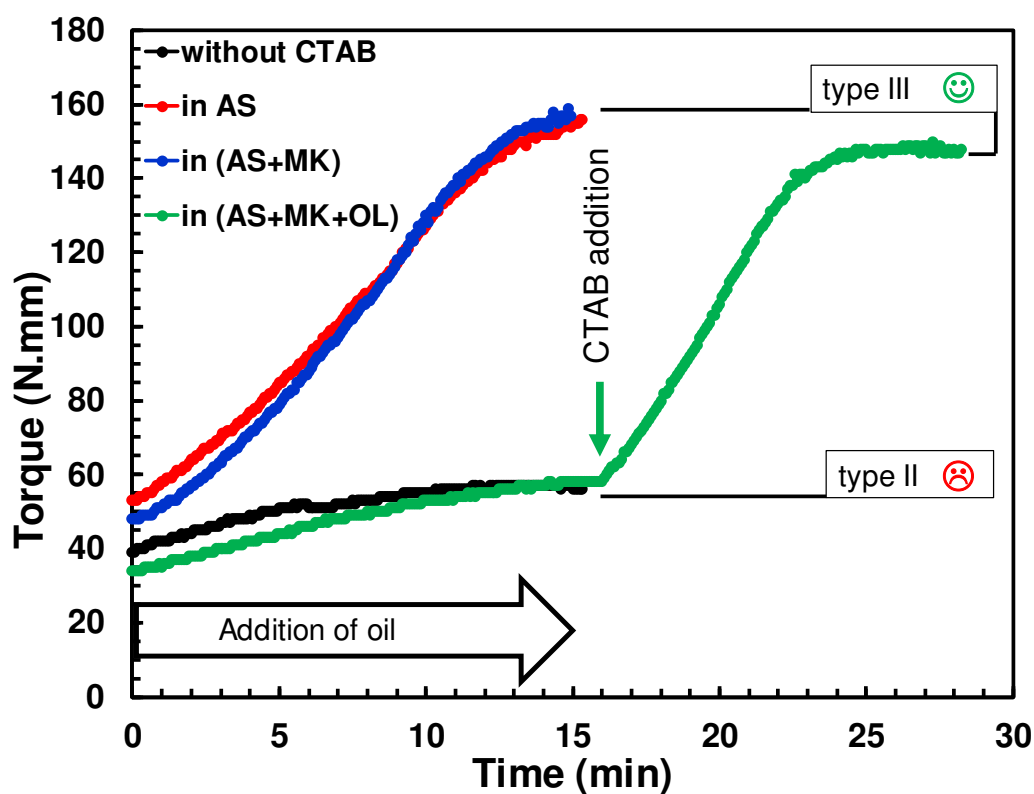

Fig. 4. Torque (N.mm) variation versus time (min) at stirring speed = 800 rpm. The addition of Finavestan (60 mL/23%) happens during the first 15 min (flow rate = 4.0 mL.min^{-1}) into 200 mL of geopolymer without CTAB (black), with introduction of 10^{-2} M CTAB in the activation solution (AS, red), after the addition of metakaolin (AS+MK, blue) and after the oil incorporation (AS+MK+oil, green). In case of AS+MK+oil, the torque is monitored during 15 additional min.

The huge increase of torque experienced when adding CTAB could be due to the adsorption of CTAB on the surface of MK particles. The polar head of CTAB is positively charged and is therefore likely to adsorb on the surface of MK particles, which are negatively charged in alkaline conditions (ZHANG and al. 2008). The hydrophobic forces arising from the interaction between hydrophobic tails of CTAB molecules cause the formation of agglomerates of MK particles (Suzzoni and al, 2018). These agglomerates are responsible for the viscosity increase due to higher effective volume. This phenomenon is even much more significant in the presence of oil, probably due to the fact that the mixture is getting close to the maximum packing fraction (E. Guazzelli and O. Pouliquen, 2018).
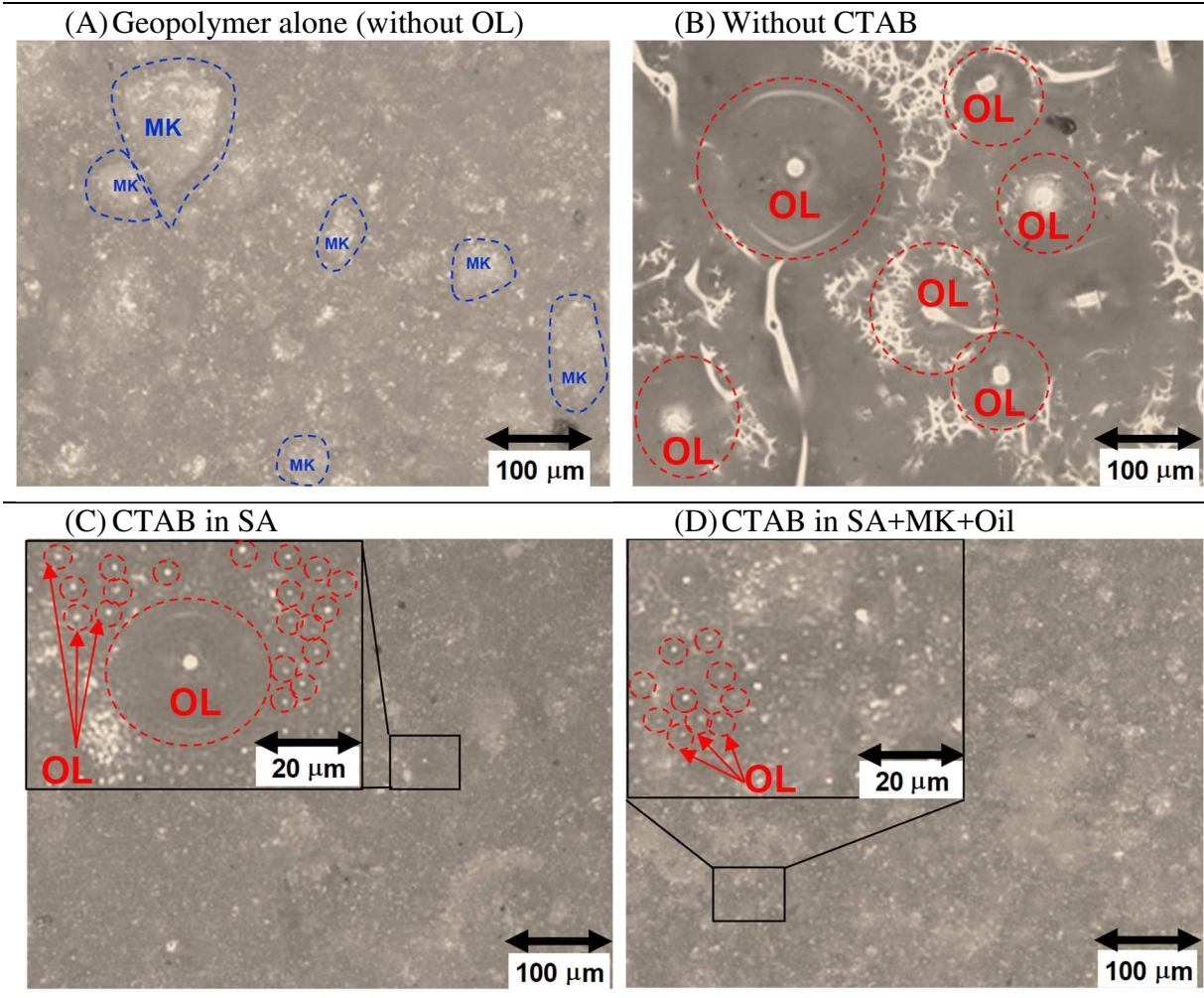

Fig. 5. Optical microscopy in reflexion mode of cured geopolymers : (**A**) without Organic Liquid (OL) and with of 23% of incorporated of Finavestan OL as described in Fig. 4 : (**B**) without CTAB, (**C**) with addition of CTAB in the activating solution and (**D**) with addition of CTAB after Finavestan incorporation.

3.5. Effect of CTAB concentration

Since the positive effect of CTAB has been shown on the incorporation of a moderately viscous oil (Fig. 4), the incorporation of a very fluid oil mixture TBP/dodecane (7/3) will be tried using CTAB. The CTAB is introduced in the activation solution at different concentrations (0, 1, 3, 5 and 10.10^{-3} M).

The black curve (Fig. 6) corresponds to the experience without CTAB. The correspondence between the torque and the viscosity was reported using the calibration curve (Fig. 1). Before oil addition, the viscosity of the GP increases with the amount of CTAB, from 1.7 Pa.s without CTAB to 3 Pa.s for 3.10^{-3} M of CTAB and to 4.5 Pa.s if 10.10^{-3} M of CTAB was used. For less important CTAB concentrations of 1.10^{-3} M and 3.10^{-3}, the torque strongly increases up to 5 mL of organic liquid added, then further increases but less quickly up to 20 mL. In the end, the quality of the dispersion is high and corresponds to a geoil type III. As previously observed, when the addition of 20 mL of oil is completed, the torque reaches a certain value (60-90 N.mm, $\approx$ 10 Pa.s) and further increases, leading to a successful incorporation. On the other hand, for the highest CTAB concentrations (5.10^{-3} M and 10.10^{-3} M), the torque increases too quickly up to 85 N.mm at just 5 mL of LO incorporated. At this stage, the viscosity is so high (around 20 Pa.s) that the rotation of the propeller can no longer drive the geopolymer from the outside towards the center of the reactor. Thus, the organic liquid can no longer penetrate inside the GP and accumulates at the surface of the slurry. In such a case, the torque signal is very noisy and the mixture heterogeneous. The torque tracking was therefore not reported on Fig. 6. A. for such high concentrations of CTAB (5.10^{-3} M and 10.10^{-3} M).

3.6. Effect of the alkyl chain length of trimethyl ammonium bromide surfactants

Several quaternary ammoniums (QA) with different chain lengths (C_6, C_8, C_{10}, C_{12}, C_{14}, C_{16}) were tested in this study. Using the results of Fig. 6. A, a QA concentration of 3.10^{-3} M was chosen for the incorporation of a TBP/dodecane mixture. Fig. 6. B shows that whatever the quaternary ammonium that is used, the oil incorporation is successful, providing with a final geoil type III, similar to the one previously obtained with CTAB (C_{16}). The torque profiles are identical for each pairs of compounds C_6-C_8, C_{10}-C_{12} and C_{14}-C_{16}-TAB. The profiles are convex for C_6-C_{12}-TAB and concave for C_{14}-C_{16}-TAB. Torque monitoring shows that quaternary ammonium with short alkyl chains such as hexamethyltrimethylammonium are able to replace CTAB for the incorporation of oil with the same efficiency. The positive action of CTAB on

the incorporation of alkane type fluids is therefore due to its positive charge rather than its than its surfactant activity.
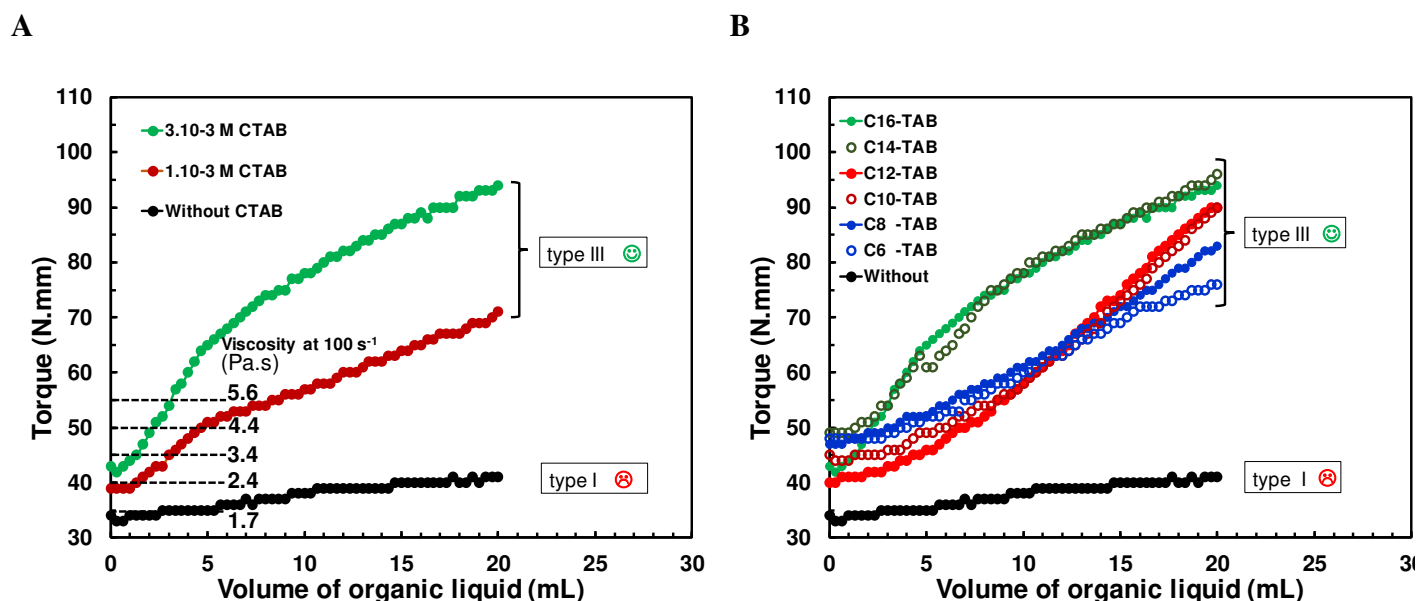
A   **B**

Fig. 6. Torque (N.mm) variation versus TBP/Dodecane volume (mL) added at a flow rate of 4.0 mL.min^{-1} at a stirring speed of 800 rpm in 80 mL of geopolymer. (**A**): Different concentrations of CTAB (0, 1, 3, 5 and 10.10^{-3} M) and (**B**): Different quaternary ammonium (C6, C8, C10, C12, C14, C16-TAB) at 3.10^{-3} M are introduced in the activating solution.

It can be observed that the magnitude of the torque increase tends to be smaller with decreasing alkyl chain length. This is in accordance with the presence of hydrophobic forces between MK particles. Shorter alkyl chains decrease the range of attraction between MK particles, which decreases the size of particles agglomerates, the effective volume and ultimately the impact on the viscosity.

3.8. Zeta potential of metakaolin particles in the presence of QA

Quaternary ammonium salts (QAs) have been used to obtain high surface area nanoporous geopolymers (Kang et al., 2005; Pei et al., 2020; Singhal et al., 2017; Yu et al., 2020) improve the compressive strength of geopolymers (Petlitckaia and Poulesquen, 2019) or to increase the hydrophobicity of mineral particles to improve the adsorption capacity of organic compounds (Chen et al., 2019; Falah et al., 2016; Montgomery et al., 1991; Siyal et al., 2018). The interaction between metakaolin and QAs, responsible for an increase in viscosity of fresh geopolymers has already been observed when using CTAB (Cantarel, 2016b; Revathi et al., 2017).

To demonstrate the interaction between metakaolin and QAs, suspensions of metakaolin in the presence of QAs with different chain lengths have been formulated and left at rest for 12 hours. This period of rest allows the QAs species to fully adsorb on the surface of the particles. Despite the fact that geopolymer formation requires very basic conditions, the range of pH was extended from 2 to 12 in this study. In the absence of QAs, the Zeta potential of metakaolin (**Fig. 7**) decreases from -10 mV to -60 mV with increasing pH value. In the presence of QAs, the Zeta potential/pH curves are strongly translated to higher values and the greater the length of the alkyl chain, the higher the value of the Zeta potential. When using CTAB, the Zeta potential is high and almost constant (60/50 mV) along de pH, even in highly alkaline conditions. These experiments demonstrate the affinity of QAs for metakaolin, and the interactions appear to be stronger with a longer alkyl chain like CTAB.
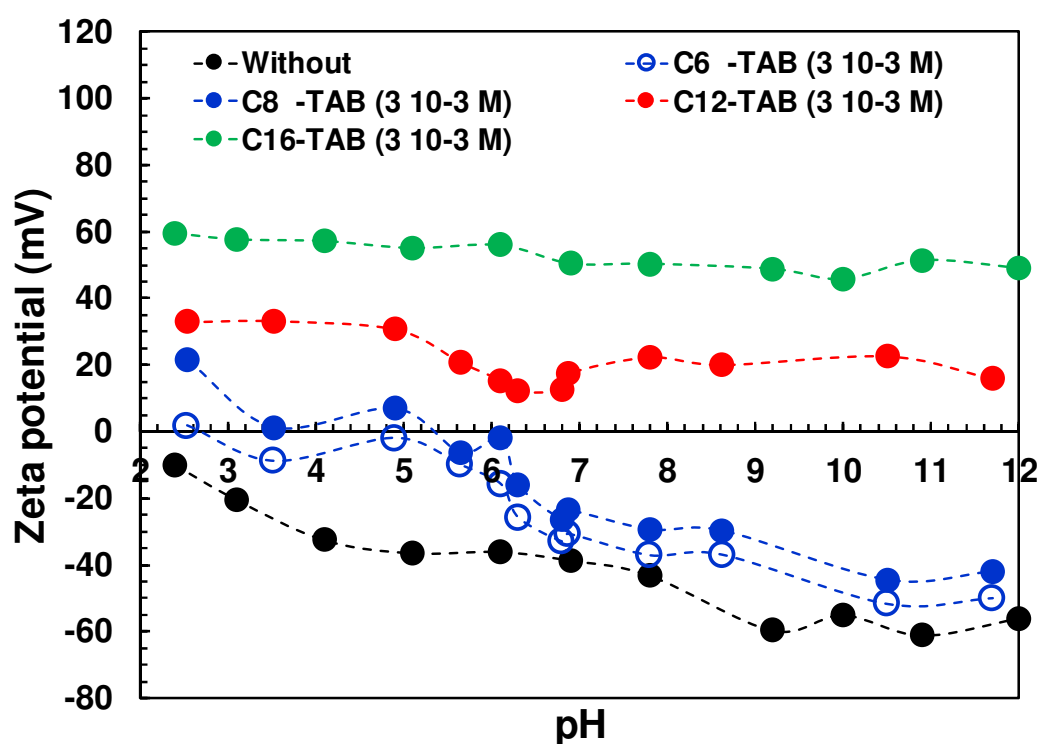

Fig. 7. Zeta potential (mV) versus pH of metakaolin suspensions without and with C_6, C_8, C_{12} and C_{16}-TAB species at 3.10^{-3} M.

The concentration of hydroxide ions in a geopolymer activation solution is about 6.75mol. L^{-1}. This high concentration of NaOH is intended to accelerate the dissolution of the Metakaolin and thus the polymerization of the geopolymer. Since the most basic conditions used in zetametry never exceeded 10^{-2} mol.L^{-1}, we considered that our basic conditions used did not influence the zeta potential measurement. Despite the fact that geopolymer formation requires very basic conditions, the range of pH was extended from 2 to 12 in this study.

3.9. Influence of the H$_2$O/Na$_2$O molar ratio (MR) without QAs

Surprisingly, it was observed that an increase in viscosity of the starting geopolymer slurry facilitates the incorporation of very fluid organic liquids such as TBP/dodecane mixtures, even in the absence of QAs. To increase the viscosity of a geopolymer slurry, the amount of water can be reduced while keeping other formulation parameters constant. The GP that serves as a reference in this study has a molar ratio (MR) H$_2$O/Na$_2$O of 13. Two others GPs with less water have been prepared (MR = 12 and MR = 11). The viscosities of the fresh geopolymers and the p ratio reported in Table 3 show that the viscosity of fresh GPs is increasing with decreasing amount of water. This is particularly observed for the formulation with the lowest amount of water (MR = 11, torque = 65 N.mm) which corresponds to a viscosity of about 10 Pa.s in comparison with 2.4 and 2.0 Pa.s for MR = 12 and 13 respectively.

During the addition of the organic liquid in the MR = 12 formulation, the torque remains slightly higher than the reference formulation MR = 13 (type I). The incorporation is therefore being slightly improved (type II) but the geoil that is obtained is still too fluid (3.5 Pa.s) to end with a high quality incorporation. In the case of the MR = 11 formulation, the torque measurement is linearly increasing with the amount of OL added and displaying a significant slope (1.7 N.mm. min^{-1}) up to 100 N.mm. In the end, the incorporation is of quality and behave as a geoil type III.
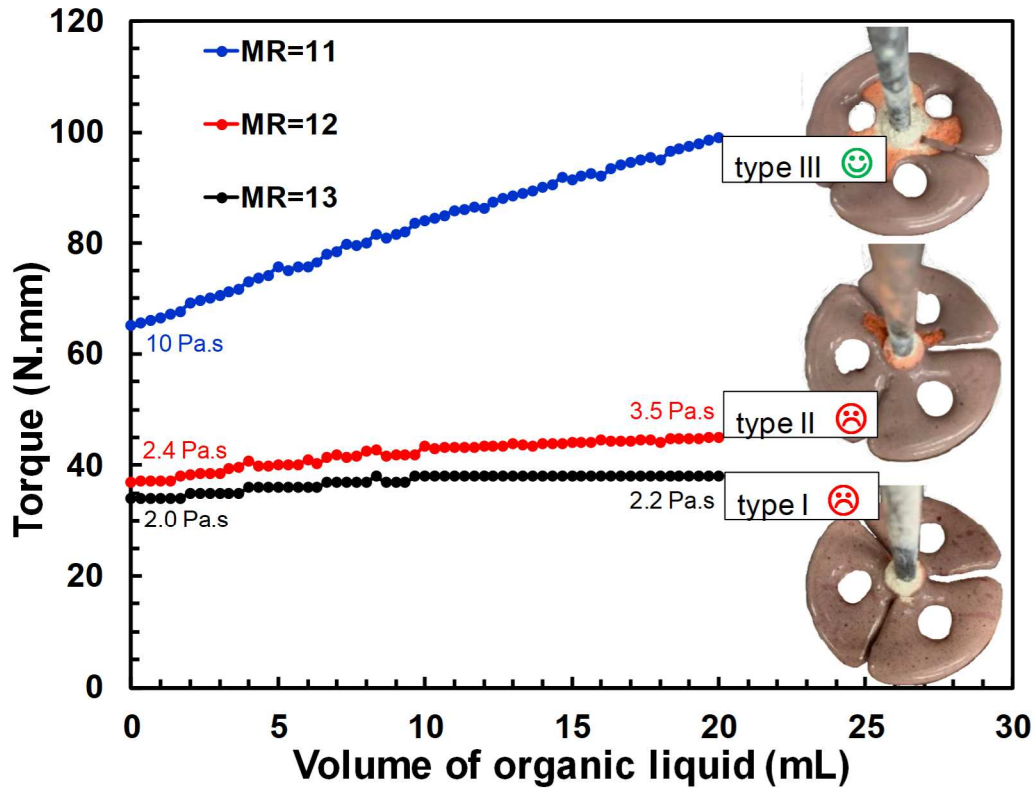
Fig. 8. Torque (N.mm) variation versus TBP/Dodecane volume (mL) added at a flow rate of 4.0 mL.min^{-1} at stirring speed = 800 rpm in 80 mL of geopolymer. Formulated with water molar ratio of 11, 12 and 13.

Table 3. Viscosity of geopolymer (Pa.s) at 25 °C at 100 s^{-1} for different H_2O/Na_2O molar ratio (MR) and corresponding p ratio (viscosity of TBP/Dodecane/ viscosity of geopolymer).

	Geopolymer		
	MR =1 3	MR = 12	MR = 11
Viscosity of geopolymer (Pa.s) at 25 °C at 100 s^{-1}	2.0	2.4	10
p ratio	1.8 10^{-3}	1.5 10^{-3}	0.36 10^{-3}

3.10. Capillary forces

The interfacial tension between TBP/Dodecane and the activating solution is the same for the three experiments presented in Fig. 8, but there is a change in the viscosity of the aqueous metakaolin suspension. The p ratio $\eta_{oil}/\eta_{Geopolymer}$ is always lower than 2.10^{-3}. According to Grace's observations (((Grace, 1982))), it is logic to consider that TBP/Dodecane cannot be incorporated as droplets into geopolymer slurries, and it is indeed the case with geopolymers (MR=12 and 13). Such observations have also been confirmed in other studies[47] in which the incorporation of dodecane in geopolymers was only possible if p is higher than 10^{-2}. Moreover, this rule seems to be verified as well for organic liquid polymers, for which the viscosity adjustment of the geopolymer slurries represents the key parameter in the process of

incorporating the resins into geopolymers (Colangelo et al., 2013). However, in the present study, the incorporation of TPB/dodecane in the MR = 11 geopolymer, for which the p ratio is the lowest (lower than 3.10^{-3}), the oil can be dispersed in a better way than for MR = 12 or 13 formulations.

To find an explanation, one has to consider that the system of interest is not just a liquid/liquid system, which would be governed by surface tension and viscosity forces only but also includes metakaolin particles. Ternary particle–liquid–liquid systems, composed of particles dispersed in two immiscible liquids can form a variety of structures depending on the ratio of the three components and their chemical affinity. Even when a tiny amount of the second immiscible liquid is added into the first liquid containing the particles (i.e. particles suspension), the rheological properties of the initial suspension can be dramatically altered from a fluid-like to a gel-like state or from a weak to a strong gel. In that case, the viscosity further increases as the volume fraction of the second fluid increases and is attributed to capillary forces between the two fluids and the solid particles. The so-called "capillary suspensions" are a typical phenomenon for these ternary systems, in which capillary or pendular states are building up depending on the wetting properties of each liquid towards the solid particles.

These capillary forces also depend on the interfacial tension between the two liquids and can be observed when the proportion of solid particles is important. This phenomenon could explain why the incorporation of TBP/dodecane is possible in a highly concentrated aqueous suspension (MR = 11) and not in a more diluted medium (MR = 12 or 13).

An experiment carried out with hydrophilic glass beads (SiO_2) in water with small amount of diisononyl phthalate (DINP) as second immiscible fluid shows that the water preferentially wets the glass beads. However, oil droplets are also wetting the glass beads to a lesser extent, but high enough to create bridges joining beads with each other, thus forming the pendular state. The same experiment with hydrophobic glass beads instead of hydrophilic ones changes the system from pendular to capillary state in which water, being the continuous phase, does not preferentially wet the treated beads (Koos, 2014; Koos and Willenbacher, 2011). Such capillary associations can be observed by microscopy using fluorescent dyes.

Unfortunately, through the course of this study, it was not possible to show such water/oil/metakaolin associations by microscopy. However, to demonstrate these capillary forces, Washburn tests were performed. Water, dodecane and Finavestan were allowed to rise along conventional and hydrophobically modified (using CTAB) metakaolin.
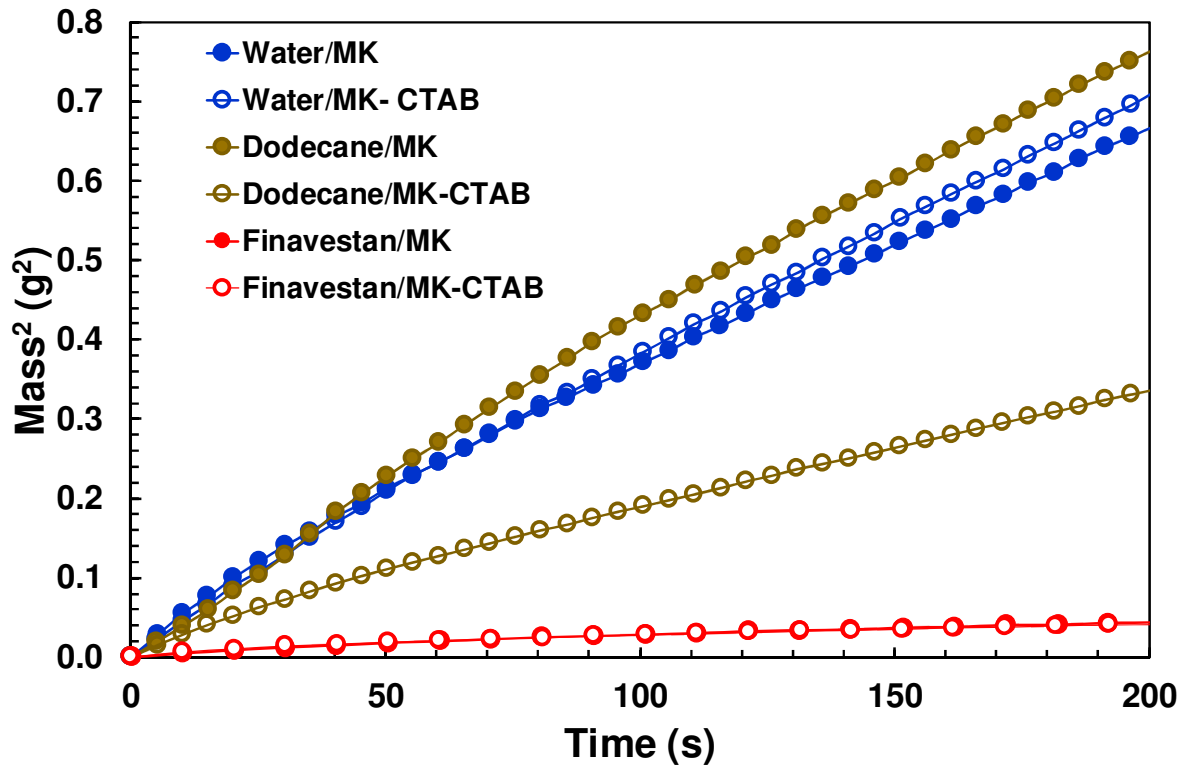
Fig. 9. Washburn tests representing the square of liquid mass (g^2) on metakaolin powders (MK) allowed to rise via capillarity in function of time. Liquids are water (blue circles), dodecane (braun circles) and Finavestan (red circles). Full circles corresponds to non-modified metakaolin and open circles to metakaolin impregnated with 10^{-2} M of CTAB.

Fig. 9 presents the results of the Washburn methods that can be described as follow. After the contact of a glass tube filled with metakaolin powder has been made, the liquid is rising along the powder as a result of capillarity, inducing an increase in mass, whose square can be plotted in function of time. If considering the metakaolin powder as a bundle of capillaries, the liquid migration into the solid can be described thanks to the Washburn equation (**Eq. 1**) below:

$$\frac{m^2}{t} = \frac{C \times \gamma \times \cos\theta \times \rho^2}{\eta} \quad (1)$$

where m, C, ρ, γ, η, θ, t are respectively the mass of liquid adsorbed, the capillary constant of the powder, the density, the superficial tension and the viscosity of the liquid, the contact angle between the liquid and the solid and the time.

Table 4. Density (kg.m^{-3}), Viscosity (Pa.s), Superficial tension (N.m^{-1}) and $\rho^2.\gamma/\eta$ (kg^2.m^{-3}.s^{-1}) at 25 °C for water, dodecane and Finavestan oil. Slope ($\Delta m^2/\Delta t$ in kg^2.s^{-1}) and C.cos(θ) are extracted from the Washburn equation.

22

Liquid	Density at 25 °C (ρ) (kg.m^{-3})	Viscosity at 25 °C (η) (Pa.s = N.s.m^{-2})	Superficial Tension at 25 °C (γ) (N.m^{-1})	$\rho^2.\gamma/\eta$ (kg^2.m^{-3}.s^{-1})	Slope ($\Delta m^2/\Delta t$) (kg^2.s^{-1})	C.cos(θ) (m^{-3})
Dodecane	749	0.0013	0.0254	3.7 10^2	3.8 10^{-9} [a] 1.6 10^{-9} [b]	1.0 10^{-7} [a] 4.3 10^{-8} [b]
Finavestan	900	0.143	0.0314	6.2 10^0	1.9 10^{-10} [a] 1.9 10^{-10} [b]	3.1 10^{-11} [a] 3.1 10^{-11} [b]
Water	1000	0.001	0.0725	5.3 10^3	3.2 10^{-9} [a] 3.5 10^{-9} [b]	6.0 10^{-7} [a] 6.0 10^{-7} [b]

[a] Slope ($\Delta m^2/\Delta t$) with metakaolin (MK), [b] with hydrophobic metakaolin (MK-CTAB)

Dodecane and water show the same migration rate in untreated metakaolin. Concerning water, the speed of migration is almost identical on the two kinds of metakaolin particles, which is not the case for dodecane, which seems to be more retained by the hydrophobic powder. About Finavestan, there is no difference in behavior depending on the nature of the metakaolin, the migration speed being rather governed by the high viscosity of the oil (**Eq. 1**), as can be confirmed by the low value of $\rho 2.\gamma / \eta$ (Table 4). From the slopes measurements ($\Delta m^2/\Delta t$) and the calculated $\rho^2.\gamma/\eta$, C.cos(θ) values can be determined (Table 4). The value of C.cos(θ) is the highest for water, followed by dodecane and finally Finavestan, which indicates that water is better wetting natural or hydrophobically treated metakaolin than dodecane or Finavestan. However, the most important observation to keep in mind for this study is that these three different liquids are capable of wetting metakaolin particles, since capillary rises are observed. The capillary interactions seen in the Washburn experiments presented in Fig. 9 bring to light the importance of the interactions between metakaolin and the two immiscible liquids. When metakaolin is impregnated with CTAB, the behavior of dodecane towards the powder changes, whereas the behavior of water remains unchanged. Thus, by concentrating an aqueous suspension of metakaolin even more, the solid-liquid interactions with the introduced oil will increase, and the strength of capillary forces will be enhanced. This could explain why the incorporation of organic liquid is made possible in very high viscosity geopolymers, even if the p ratio is lower than 10^{-3} (Fig. 8).

Conclusion

Torque monitoring, which is very convenient in the case of industrial applications, was used to follow the incorporation of OL in geopolymer. First, in-line torque monitoring during OL incorporation into geopolymer (GP) slurries provides information on the viscosity of the mixtures using a prior calibration. This avoids off-line rheological measurements and allows observing the impact of each components on the rheology of the mixtures. In addition, in-line torque monitoring allows having relevant information about the OL incorporation process. In particular, three types of torque evolution were identified upon OL addition, corresponding to three types of fresh GEOIL textures (Type I, II and III). When the OL is not incorporated and remains at the surface of the geopolymer slurry, the torque remains constant, which corresponds to Type I GEOIL. On the contrary, effective OL incorporation processes are those displaying an increase in torque. If the torque increases at the start of OL incorporation, but remains constant from a specific amount of OL incorporated, Type II GEOIL is obtained, with an excess of OL at the surface of the mixture. In order to obtain a continuous increase in torque, corresponding to a full incorporation of the OL, the addition of quaternary alkylammonium (QAs) has proven to be very efficient (Type III). It was demonstrated that the effectiveness of QAs is due to the positive charge of the quaternary ammonium part rather than to the length of the alkyl chain. More specifically, QAs species increase the viscosity of fresh GP and act on the viscosity ratio (p) between the OL and the GP. This ratio is an important parameter to obtain a suitable OL incorporation (Type III). In accordance with Grace's observations, a ratio greater than 10^{-2} constitutes favorable conditions. However, even at very low p ratio ($< 10^{-3}$), when highly viscous geopolymers are used (MR = 11), the incorporation of OL is possible. In that case, metakaolin particles (MK) are concentrated enough to consider the presence of strong particle/liquid interactions. These capillary forces were demonstrated using the Washburn method, showing different behavior between OL, water and MK particles, depending on whether the latter has been hydrophobically treated with QAs or not.

The alkali-activation of metakaolin, poor in Ca, leads to the formation of a 3D reticulated alumino-silicate gel (N-A-S-H), the so-called geopolymer structure. Other raw materials used for alkali-activation, rich in Ca (e.g. fly ash C or slag) lead to the formation of 2D calcium alumino-silicate hydrates (C-A-S-H) as in Portland cements. This type of material is less suitable for OL immobilization. On the contrary, the literature reports the very good compatibility of various organic liquids with geopolymer materials (Reeb et al., 2021). It would

indeed be interesting to investigate other Ca-poor raw materials with the purpose of recycling industrial wastes (e.g. fly ash F, red mud). However, metakaolin (MK) was chosen in this study for its stable composition and easy supply.

In conclusion, the in-line torque monitoring is useful to ensure OL incorporation (i.e. when the torque increases) but also to maintain sufficient workability of the final GEOIL mixture. The addition of QAs surfactants is required for the incorporation of some OL in fresh GP. It can be noticed that QAs can be added directly in the activation solution or after the OL incorporation step with no significant differences. However, the addition of QAs leads to a strong viscosity increase of fresh GEOIL, which can be an issue at an industrial scale. In this work, only QAs surfactants were tested and other types should be considered to better control the rheology of GEOIL mixtures. Finally, in the case of successful OL incorporation (Type III), droplets are efficiently dispersed and smaller than 10 microns in the GEOIL composite.

References

Akay, G., 1997. Flow-induced phase inversion in the intensive processing of concentrated emulsions. Chem. Eng. Sci. 53, 203–223. https://doi.org/10.1016/S0009-2509(97)00199-1

Akay, G., Tong, L., 2001. Preparation of Colloidal Low-Density Polyethylene Latexes by Flow-Induced Phase Inversion Emulsification of Polymer Melt in Water. J. Colloid Interface Sci. 239, 342–357. https://doi.org/10.1006/jcis.2001.7615

Allouche, J., Tyrode, E., Sadtler, V., Choplin, L., Salager, J.-L., 2004. Simultaneous Conductivity and Viscosity Measurements as a Technique To Track Emulsion Inversion by the Phase-Inversion-Temperature Method. Langmuir 20, 2134–2140. https://doi.org/10.1021/la035334r

Autef, A., Joussein, E., Poulesquen, A., Gasgnier, G., Pronier, S., Sobrados, I., Sanz, J., Rossignol, S., 2013. Influence of metakaolin purities on potassium geopolymer formulation: The existence of several networks. J. Colloid Interface Sci. 408, 43–53. https://doi.org/10.1016/j.jcis.2013.07.024

Bai, C., Colombo, P., 2018. Processing, properties and applications of highly porous geopolymers: A review. Ceram. Int. 44, 16103–16118. https://doi.org/10.1016/j.ceramint.2018.05.219

Bai, C., Franchin, G., Elsayed, H., Conte, A., Colombo, P., 2016. High strength metakaolin-based geopolymer foams with variable macroporous structure. J. Eur. Ceram. Soc. 36, 4243–4249. https://doi.org/10.1016/j.jeurceramsoc.2016.06.045

Barbosa, T.R., Foletto, E.L., Dotto, G.L., Jahn, S.L., 2018. Preparation of mesoporous geopolymer using metakaolin and rice husk ash as synthesis precursors and its use as potential adsorbent to remove organic dye from aqueous solutions. Ceram. Int. 44, 416–423. https://doi.org/10.1016/j.ceramint.2017.09.193

Cantarel, V., 2016. Etude de la synthèse de composites liquides organiques/géopolymère en vue du conditionnement de déchets nucléaires. Université Blaise Pascal-Clermont-Ferrand II.

Cantarel, V., Lambertin, D., Poulesquen, A., Leroux, F., Renaudin, G., Frizon, F., 2018. Geopolymer assembly by emulsion templating: Emulsion stability and hardening mechanisms. Ceram. Int. 44, 10558–10568. https://doi.org/10.1016/j.ceramint.2018.03.079

Cantarel, V., Nouaille, F., Rooses, A., Lambertin, D., Poulesquen, A., Frizon, F., 2015. Solidification/stabilisation of liquid oil waste in metakaolin-based geopolymer. J. Nucl. Mater. 464, 16–19. https://doi.org/10.1016/j.jnucmat.2015.04.036

Catte, M., Ontiveros, J.F., Aramaki, K., Pierlot, C., 2018. Catastrophic emulsion inversion process of highly viscous isosorbide biobased polyester monitored in situ by torque and light backscattering. J. Oleo Sci. 67, 925–931. https://doi.org/10.5650/jos.ess18057

Chen, S., Qi, Y., Cossa, J.J., Salomao, D.S.I.D., 2019. Efficient removal of radioactive iodide anions from simulated wastewater by HDTMA-geopolymer. Prog. Nucl. Energy 117, 103112. https://doi.org/10.1016/j.pnucene.2019.103112

Cilla, M.S., de Mello Innocentini, M.D., Morelli, M.R., Colombo, P., 2017. Geopolymer foams obtained by the saponification/peroxide/gelcasting combined route using different soap foam precursors. J. Am. Ceram. Soc. 100, 3440–3450. https://doi.org/10.1111/jace.14902

Colangelo, F., Roviello, G., Ricciotti, L., Ferone, C., Cioffi, R., 2013. Preparation and characterization of new geopolymer-epoxy resin hybrid mortars. Materials 6, 2989–3006.

Davidovits, J., 1991. Geopolymers: inorganic polymeric new materials. J. Therm. Anal. 37, 1633–56.

Davy, C.A., Hauss, G., Planel, B., Lambertin, D., 2019. 3D structure of oil droplets in hardened geopolymer emulsions. J. Am. Ceram. Soc. 102, 949–954. https://doi.org/10.1111/jace.16142

Dusserre, G., Farrugia, A., Cutard, T., 2020. Rheology evolution of a geopolymer precursor aqueous suspension during aging. Int. J. Appl. Ceram. Technol. Ahead of Print. https://doi.org/10.1111/ijac.13508

Duxson, P., Fernandez-Jimenez, A., Provis, J.L., Lukey, G.C., Palomo, A., Deventer, J.S.J., 2007. Geopolymer technology: The current state of the art. J. Mater. Sci. 42, 2917–2933. https://doi.org/10.1007/s10853-006-0637-z

Edward, A.C., Veronique, S., Philippe, M., Lionel, C., Frederic, D., Michel, M., 2014. Preparation of highly concentrated bitumen emulsions by catastrophic phase inversion: Follow-up of the emulsification process. Colloids Surf., A 458, 25–31. https://doi.org/10.1016/j.colsurfa.2014.02.030

Falah, M., MacKenzie, K.J., Knibbe, R., Page, S.J., Hanna, J.V., 2016. New composites of nanoparticle Cu (I) oxide and titania in a novel inorganic polymer (geopolymer) matrix for destruction of dyes and hazardous organic pollutants. Journal of hazardous materials 318, 772–782.

Galindo-Alvarez, J., Sadtler, V., Choplin, L., Salager, J.-L., 2011. Viscous Oil Emulsification by Catastrophic Phase Inversion: Influence of Oil Viscosity and Process Conditions. Ind. Eng. Chem. Res. 50, 5575–5583. https://doi.org/10.1021/ie102224k

Glad, B.E., Kriven, W.M., 2015. Highly Porous Geopolymers Through Templating and Surface Interactions. J. Am. Ceram. Soc. 98, 2052–2059. https://doi.org/10.1111/jace.13584

Goger, A., Thompson, M.R., Pawlak, J.L., Lawton, D.J.W., 2015. In Situ Rheological Measurement of an Aqueous Polyester Dispersion during Emulsification. Ind. Eng. Chem. Res. 54, 5820–5829. https://doi.org/10.1021/acs.iecr.5b00765

Grace, H.P., 1982. Dispersion phenomena in high viscosity immiscible fluid systems and application of static mixers as dispersion devices in such systems. Chemical Engineering Communications 14, 225–277.

Guazzelli, E., Pouliquen, O., 2018. Rheology of dense granular suspensions. J. fluid mech. 852, P1/1-P1/73. https://doi.org/ 10.1017/jfm.2018.548

Hussain, M., Varely, R., Cheng, Y.B., Mathys, Z., Simon, G.P., 2005. Synthesis and thermal behavior of inorganic-organic hybrid geopolymer composites. J. Appl. Polym. Sci. 96, 112–121. https://doi.org/10.1002/app.21413

Hussain, M., Varley, R.J., Cheng, Y.B., Simon, G.P., 2004. Investigation of thermal and fire performance of novel hybrid geopolymer composites. J. Mater. Sci. 39, 4721–4726. https://doi.org/10.1023/B:JMSC.0000034180.35216.ba

Kang, F., Wang, Q., Xiang, S., 2005. Synthesis of mesoporous Al-MCM-41 materials using metakaolin as aluminum source. Materials Letters 59, 1426–1429.

Koos, E., 2014. Capillary suspensions: Particle networks formed through the capillary force. Current opinion in colloid & interface science 19, 575–584.

Koos, E., Willenbacher, N., 2011. Capillary forces in suspension rheology. Science 331, 897–900.

Lambertin, D., Cantarel, V., Poulesquen, A., Frizon, F., 2018. Production of geopolymer composites comprising organic phase change materials.

Liu, J., Li, F., Zhang, R., Dong, E., Gong, X., Lun, Y., Zhang, T., Zhu, J., 2018. Foam geopolymer for tunnel composite lining and preparation method thereof.

Medpelli, D., Seo, J.-M., Seo, D.-K., 2014. Geopolymer with Hierarchically Meso-/Macroporous Structures from Reactive Emulsion Templating. J. Am. Ceram. Soc. 97, 70–73. https://doi.org/10.1111/jace.12724

Montgomery, D.M., Sollars, C.J., Perry, R., 1991. Optimization of cement-based stabilization/solidification of organic-containing industrial wastes using organophilic clays. Waste management & research 9, 21–34.

Pei, Y.-R., Yang, J.-H., Choi, G., Choy, J.-H., 2020. A geopolymer route to micro- and meso-porous carbon. RSC Adv. 10, 6814–6821. https://doi.org/10.1039/C9RA09698A

Petlitckaia, S., Poulesquen, A., 2019. Design of lightweight metakaolin based geopolymer foamed with hydrogen peroxide. Ceramics International 45, 1322–1330.

Pierlot, C., Ontiveros, J.F., Royer, M., Catte, M., Salager, J.-L., 2018. Emulsification of viscous alkyd resin by catastrophic phase inversion with nonionic surfactant. Colloids Surf., A 536, 113–124. https://doi.org/10.1016/j.colsurfa.2017.07.030

Provis, J.L., van Deventer, J.S.J., Editors., 2009. Geopolymers: Structure, Processing, Properties and Industrial Applications. Woodhead Publishing Ltd.

Reeb, C., Pierlot, C., Davy, C., Lambertin, D., 2021. Incorporation of organic liquids into geopolymer materials-A review of processing, properties and application. Ceram. Int. 47, 7369-7385.https://doi.org/ 10.1016/j.ceramint.2020.11.239

Revathi, T., Jeyalakshmi, R., Rajamane, N.P., Sivasakthi, M., 2017. Evaluation of the role of Cetyltrimethylammoniumbromide (CTAB) and Acetylenicglycol (AG) admixture on fly ash based geopolymer. Orient J Chem 33, 783–792.

Rouyer, J., Poulesquen, A., 2015. Evidence of a Fractal Percolating Network During Geopolymerization. J. Am. Ceram. Soc. 98, 1580–1587. https://doi.org/10.1111/jace.13480

Saw, L.K., Brooks, B.W., Carpenter, K.J., Keight, D.V., 2004. Catastrophic phase inversion in region II of an ionomeric polymer-water system. J. Colloid Interface Sci. 279, 235–243. https://doi.org/10.1016/j.jcis.2004.06.056

Singhal, A., Gangwar, B.P., Gayathry, J.M., 2017. CTAB modified large surface area nanoporous geopolymer with high adsorption capacity for copper ion removal. Applied Clay Science 150, 106–114.

Siyal, A.A., Shamsuddin, M.R., Khan, M.I., Rabat, N.E., Zulfiqar, M., Man, Z., Siame, J., Azizli, K.A., 2018. A review on geopolymers as emerging materials for the adsorption of heavy metals and dyes. Journal of Environmental Management 224, 327–339.

Song, D., Zhang, W., Gupta, R.K., Melby, E.G., 2011. Role of operating conditions in determining droplet size and viscosity of tackifier emulsions formed via phase inversion. AIChE J. 57, 96–106. https://doi.org/10.1002/aic.12238

Steins, P., Poulesquen, A., Diat, O., Frizon, F., 2012. Structural Evolution during geopolymerization from an Early Age to Consolidated Material. Langmuir 28, 8502–8510. https://doi.org/10.1021/la300868v

Sun, C., Xiang, J., Xu, M., He, Y., Tong, Z., Cui, X., 2020. 3D extrusion free forming of geopolymer composites: Materials modification and processing optimization. J. Cleaner Prod. 258, 120986. https://doi.org/10.1016/j.jclepro.2020.120986

Suzzoni, A., Barre, L., Kohler, E., Levitz, P., Michot, L. J., M'Hamdi, J.2018. Interactions between kaolinite clay and AOT. Coll. Surf. A:, 556, 309-315. https://doi.org/10.1016/j.colsurfa.2018.07.049

Thakur, N., Weatherly, C.A., Wimalasinghe, R.M., Armstrong, D.W., 2019. Fabrication of interconnected macroporosity in geopolymers via inverse suspension polymerization. J. Am. Ceram. Soc. 102, 4405–4409. https://doi.org/10.1111/jace.16437

Wang, S., Ma, X., He, L., Zhang, Z., Li, L., Li, Y., 2019. High strength inorganic-organic polymer composites (IOPC) manufactured by mold pressing of geopolymers. Construction and Building Materials 198, 501–511.

Yu, Z., Song, W., Li, J., Li, Q., 2020. Improved simultaneous adsorption of Cu (II) and Cr (VI) of organic modified metakaolin-based geopolymer. Arabian Journal of Chemistry 13, 4811–4823.

Yunsheng, Z., Wei, S., Zongjin, L., Xiangming, Z., Eddie, Chungkong, C., 2008. Impact properties of geopolymer based extrudates incorporated with fly ash and PVA short fiber. Construction and Building Materials 22, 370–383. https://doi.org/10.1016/j.conbuildmat.2006.08.006

Zhang, X.P., Hu, Y.H., Liu, R.Q., 2008. J. Cent. South Univ. Tech. ing Hydrophobic aggregation of ultrafine kaolinite 15, 368-372. https://doi.org/10.1007/s11771-008-0069-9